

SHOW-THROUGH CANCELLATION IN SCANNED IMAGES USING BLIND SOURCE SEPARATION TECHNIQUES

Boaz Ophir* and David Malah

Department of Electrical Engineering
Technion - Israel Institute of Technology
email: boazo@il.ibm.com; malah@ee.technion.ac.il

ABSTRACT

Show-Through is a common occurrence when scanning duplex printed documents. The back-side printing shows through the paper, contaminating the front side image. Previous work modeled the problem as a *non-linear convolutive mixture* of images and offered solutions based on decorrelation. In this work we propose a cleaning process based on a Blind Source Separation approach. We define a cost function incorporating the non-linear mixing model in a mean-squared error term, along with a regularization term based on Total-Variation. We propose a location dependent regularization tradeoff, preserving image edges while removing show-through edges. The images and mixing parameters are estimated using an alternating minimization process, with each stage using only convex optimization methods. The resulting images exhibit significantly lower show-through, both visibly and in objective measures.

Index Terms— Image Separation, Scanned Images, BSS, Total-Variation, ICM

1. INTRODUCTION

Cross talk (or show-through) interference is a common occurrence when scanning duplex printed documents. The back-side printing shows through the paper thus contaminating the front side image. The same occurs when scanning the reverse side of the page. This may not be a problem in low quality scans (as done in home/office scanners) where, up to a degree, image quality is not an issue. The matter becomes crucial when the show-through effect is significant due to the use of very thin paper or when image quality is essential. Such is the case when creating a master copy in the digital printing industry.

Previous work [1] focused on analyzing the process that causes the phenomena, tracking the passage of light in the scanner mechanism as it passes through the document (see Fig. 1), creating a physical model for it and trying to linearize

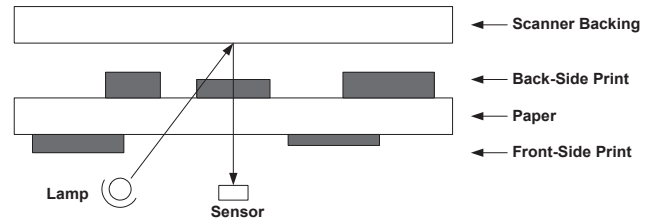


Fig. 1. Passage of light through a duplex printed document.

it. Thus, the show-through problem can be modelled as a linear convolutive mixture of non-linear transformations of the desired images.

In [1], and in our previous work [2], the cleaning process, based on the developed model, applies Least-Squares adaptive filtering techniques to estimate the point spread function and clean the front-side image, using the back-side image as a reference noise signal, and vice versa.

In our current work we approach the problem as a Blind Source Separation (BSS) problem, simultaneously estimating the images and mixing parameters. Our image separation process is based on the minimization of a cost functional. We combine a Mean Squared Error fidelity term, incorporating the *non-linear* mixing model, and Total-Variation (TV) regularization terms, applied separately to each image. A novel location dependent weighting scheme insures simultaneous true edge preservation while reducing show-through induced edges. Optimization is done alternately on the images and on the mixing parameters. This allows us to use only convex optimization techniques. Applying the ICM optimization method [3] further simplifies the process.

The resulting images exhibit significantly lower show-through both, visibly and in objective measures such as cross-correlation and mutual information.

2. COST FUNCTION

We denote by \mathbf{X} the measured mixed images, by \mathbf{Y} the estimated separated images, and by \mathcal{H} the estimated mixing operator:

$$\mathcal{H} = \begin{bmatrix} 1 & \mathbf{h}_1 * f(\cdot) \\ \mathbf{h}_2 * f(\cdot) & 1 \end{bmatrix}, \quad (1)$$

*B. Ophir is a research staff member at the IBM Haifa Research Lab.

where h_i are point-spread functions modeling the diffraction of light as it passes through the paper, and $f(\cdot)$ a *known* non-linear transformation [1, 2]. The determination of \mathbf{Y} and \mathcal{H} becomes a minimization problem, as follows:

$$(\hat{\mathbf{Y}}, \hat{\mathcal{H}}) = \arg \min_{\mathbf{Y}, \mathcal{H}} \|\mathcal{H}(\mathbf{Y}) - \mathbf{X}\|_2^2 + \lambda \text{TV}(\mathbf{Y}), \quad (2)$$

where $\text{TV}(\mathbf{Y})$ denotes the total variation operator:

$$\text{TV}(s) \equiv \int |\nabla s| dx dy \equiv \int \sqrt{s_x^2 + s_y^2} dx dy, \quad (3)$$

where s_x and s_y denote the image derivatives in the x and y axes, respectively. The term λ determines the tradeoff between fidelity and regularization. In the BSS framework the underlying assumption of the *independence* of the mixed images allows us to decompose the regularization term into a sum of two independent terms, one for each image:

$$\text{TV}(\mathbf{Y}) = \text{TV}(y_1) + \text{TV}(y_2) \quad (4)$$

The TV measure has the advantage of being both convex and edge preserving. This approach has been found to be especially good in preserving sharp edges while not penalizing smooth images [4].

We use the following discretization of (4), as proposed in [5], where the gradient field is computed on points in between pixel locations, at half pixel horizontal/vertical shifts:

$$\text{TV}(s) = \frac{1}{2} \left[\sum_{i=1}^{n-1} \sum_{j=1}^n \sqrt{[s_x(i + \frac{1}{2}, j)]^2 + [s_y(i + \frac{1}{2}, j)]^2} + \sum_{i=1}^n \sum_{j=1}^{n-1} \sqrt{[s_x(i, j + \frac{1}{2})]^2 + [s_y(i, j + \frac{1}{2})]^2} \right] \quad (5)$$

Additional penalty terms can be added to the cost functional, incorporating additional prior knowledge.

2.1. Location Dependent λ for Image Separation

An important issue is the tradeoff between the relative strengths of the fidelity term and the regularization term, determined by the parameter λ . This is particularly true in image processing applications. In [5] Strong *et al* propose using a varying, location dependent, weight term, for the purpose of image denoising. Under their scheme, a high weight is assigned to the regularization term in smooth image areas, and a low one at image edges.

Thus, strong denoising can be achieved while simultaneously preserving image edges.

Since we are dealing with an image separation scenario, the tradeoff term λ can be set separately for each image. Furthermore, in this scenario additional considerations need to be

taken in determining the location dependent tradeoff, since the interference component in each image is itself derived from the second image. Thus the interference itself contains edges that we want to overcome in the total variation minimization process. We therefore want to recognize these interference edges (as opposed to the desired edges). We assign a high weight to the regularization term in these regions thus smoothing them out. At true image edges we will choose a low value of λ so as to preserve the edge. In addition, since the backside image is slightly blurred, the back-side edges affect not only the front-side pixels at their exact location, but also pixels in their vicinity.

Based on these guidelines we propose the following weighting scheme that uses both front and back-side reconstructed images y_1 and y_2 . Two weight maps λ^1 and λ^2 are created each with components in the x and y directions. The x component is applied to the first part of (5) and the y component to the second.

If $|y_{2x}(i, j)| < c * |y_{1x}(i, j)|$:

$$\lambda_x^1(i, j) = \frac{1}{|y_{1x}(i, j)|} \quad (6)$$

else (edge is a result of show-through):

$$\lambda_x^1(i, j) = |y_{2x}(i, j)|, \quad (7)$$

where y_{1x} and y_{2x} denote gradient images (in the x direction), diluted by a small structuring image (such as 3×3). The purpose of the gray-scale dilation is to insure that the edge pixels affect not only their exact location, but their immediate vicinity as well. c is an estimated attenuation factor. We found that setting c to values in the range of 5-10 proved adequate in our examples.

The y component of the weight maps is set similarly using the y direction component of the gradient. The weight map for the reverse side image is created in a similar manner.

Fig. 2 depicts an example of the horizontal weighting maps (λ_x). Notice the low (dark) values along edges with vertical components, such as along the edges of the letters "i" and "n" in the front-side image (b). Notice however, that the show-through edges do not have the same effect. Areas affected by show-through, as well as smooth areas, all have relatively higher (brighter) values, as can be seen in (d).

Recalculating the weighting maps during the optimization process serves to further reinforce the show-through removal. As the show-through edge is gradually removed, λ at the edge will increase (since it is inversely proportional to the show-through edge strength), thus reinforcing the removal.

3. OPTIMIZATION FRAMEWORK

The minimization process (2) in the joint solution space $\{\mathbf{Y}, \mathcal{H}\}$ is a very difficult problem. The optimization problem is both non-linear and non-convex in the joint solution space, requiring specialized optimization tools. Therefore, we do not solve

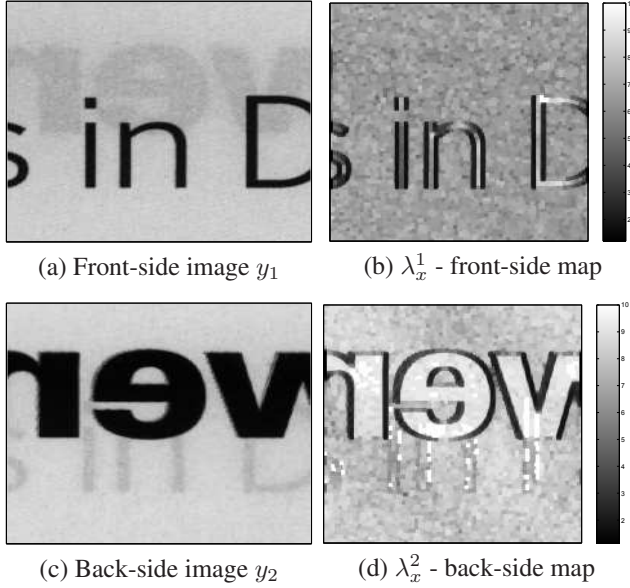


Fig. 2. Weighting maps example.

the problem directly. Instead, we approach the joint MAP estimation by an alternating minimization scheme. This popular complexity reduction approach consists of iterative alternating estimation steps with respect to the different sets of variables.

The optimization process we use consists of alternating minimization stages in \mathbf{Y} - the recovered images while keeping the mixing parameters constant, and \mathcal{H} - the convolutive mixing parameters, while keeping the images constant.

$$\hat{\mathbf{Y}} = \arg \min_{\mathbf{Y}} \{ \|\mathcal{H}(\mathbf{Y}) - \mathbf{X}\|_2^2 + \lambda TV\{\mathbf{Y}\} \} \quad (8)$$

$$\hat{\mathcal{H}} = \arg \min_{\mathcal{H}} \{ \|\mathcal{H}(\mathbf{Y}) - \mathbf{X}\|_2^2 \} \quad (9)$$

Although the cost function is non-convex in the joint space $\{\mathbf{Y}, \mathcal{H}\}$, by choosing a convex regularization term, such as TV, the cost function becomes convex in both \mathbf{Y} and \mathcal{H} separately. The \mathbf{Y} minimization stage (8) is clearly convex as both the MSE term and the TV term are each convex in \mathbf{Y} . The \mathcal{H} minimization stage (9) is also clearly convex in \mathcal{H} .

Thus, each optimization stage uses only simple convex optimization techniques. This is in contrast to [6] where the use of non-convex MRF regularization functionals requires the use of specially tailored non-convex optimization tools.

While this reduction makes the optimization more feasible, the optimization process is still burdensome. The \mathbf{Y} optimization stage is especially problematic. The large number of interrelated variables (all the pixels in both images) pose a computational challenge.

3.1. \mathbf{Y} Minimization - Iterated Conditional Modes

As explained above, the many dependent variables (all the image pixels for both front and back sides) cause the image es-

timization stage to be cumbersome. Furthermore, image models, such as MRFs, assume certain local image characteristics, while a global optimization process may induce undesirable large scale properties of the random field. To solve these problems Besag [3] offers the Iterated Conditional Modes (ICM) algorithm, an iterative method for image reconstruction that does not depend on large scale characteristics.

In the ICM method, pixel locations are visited sequentially. At each step the pixel value is updated as to minimize the image cost, with all other pixel values held constant. When applied sequentially to all the pixels, this procedure defines a single cycle of the algorithm. Typically, convergence occurs after only a few such iterations to a local image probability maximum.

Applying this method to the image separation problem, each location consists of a pixel pair (front and back side pixels at that location) to be changed.

An advantage of this method is that during each pixel optimization we need not calculate the complete cost function. Instead, due to the local nature of the pixel relations, we need to apply minimization only to the parts of the cost function that are affected by the current location.

3.2. \mathcal{H} minimization

The \mathcal{H} optimization step is much simpler due to the smaller number of variables. Given no prior knowledge on the mixing parameters this problem becomes a Least-Squares problem minimizing only the fidelity term (9). Using all pixel information (the whole two images) may hinder the solution as many non-informative pixels introduce noise to the process. We want to evaluate the PSFs by only using locations with single-side activity. An active pixel is one with significant print in its vicinity. This is determined by comparing the minimum value of neighboring pixels to a certain threshold, which is dependent on the brightness of unprinted paper [2]. A binary *activity mask*, M , is incorporated in the fidelity term so that only the relevant pixels contribute to the cost function.

As in [2] we use a cascaded approach starting with small PSF support and increasing the support in latter iterations.

4. PROPOSED ALGORITHM

To summarize, the proposed algorithm is:

1. Initialize $\mathbf{Y} = \mathbf{X}$ and $\mathcal{H} = \begin{bmatrix} 1 & \epsilon \\ \epsilon & 1 \end{bmatrix}$, $\epsilon \sim 0.1$
2. Alternating minimization stage:

(a) \mathbf{Y} optimization:

- i. Compute tradeoff maps $\lambda^{1,2}(m, n)$
- ii. ICM iterations until convergence - each iteration includes two scans: forward and reverse.

For each pixel location minimize:

$$\{\hat{y}_1(m, n), \hat{y}_2(m, n)\} = \arg \min_{y_{1,2}(m,n)} \{\|\mathcal{H}(\mathbf{Y}) - \mathbf{X}\|_2^2 + \lambda TV\{\mathbf{Y}\}\}_{(m,n)}$$

Minimization is done by a line-search process and is done only on the elements of the cost function dependent on location (m, n) .

(b) \mathcal{H} optimization:

- i. Compute activity masks M
- ii. Least-Squares minimization:

$$\hat{\mathcal{H}} = \arg \min_{\mathcal{H}} \{\|M(\mathcal{H}(\mathbf{Y}) - \mathbf{X})\|_2^2\}$$

Alternate repeatedly between stages 2a and 2b until convergence (or for a predetermined number of iterations).

3. Repeat stage 2 with a larger PSF support. This can be done several times with predetermined support for each iteration.

An additional penalty term can be added to the \mathbf{Y} minimization stage, penalizing pixel values brighter than the local background brightness, as computed in [2].

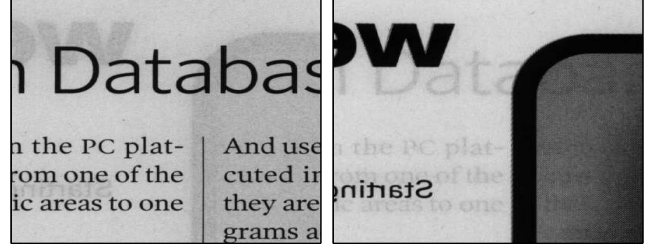
5. RESULTS

The original scanned images are shown in Fig. 3. We can get a feel of the amount of show-through by measuring the similarity of the front and back side images. The measures for these images are Normalized Cross Correlation $XC = 0.323$ and Mutual Information $MI = 0.153$.

We ran 4 alternating minimization stages. Each ICM stage took 3-5 iterations. Filter support of 1×1 was used in the first stage and 5×5 in the latter stages. The algorithm's results are shown in Fig. 4. A significant reduction in show-through is clearly seen. After cleaning, the similarity measures are $XC = 0.056$ and $MI = 0.129$. Still, it should be mentioned that these objective measures are limited in describing the show-through effect, as in our experiments we didn't find sufficient match between image quality and the degree of improvement in the measures.

6. CONCLUSION

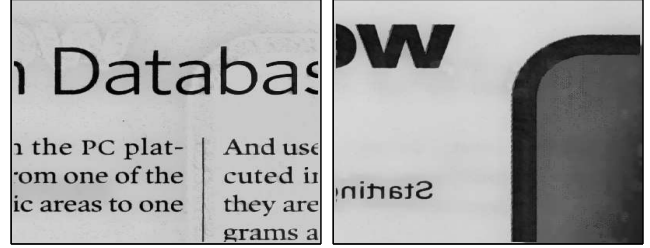
In this article we showed how the BSS framework can be used for separating complicated image mixtures as demonstrated in the considered show-through problem, where the scanned images are a non-linear convolutive mixture of images. We use Total-Variation regularization coupled with a novel location dependent scheme for setting the trade-off terms. We thus achieve good edge preservation, while avoiding the use non-convex functions and optimization methods. Applying



(a) Front

(b) Back

Fig. 3. Scanned images.



(a) Front

(b) Back

Fig. 4. Cleaned images.

the ICM optimization method further simplifies the process. The combination of all these methods is found to give good show-through cancellation.

7. REFERENCES

- [1] G. Sharma, "Show-Through Cancellation in Scans of Duplex Printed Documents," *IEEE Transactions on Image Processing*, vol. 10, no. 5, pp. 736–754, May 2001.
- [2] B. Ophir and D. Malah, "Improved Cross-Talk Cancellation in Scanned Images by Adaptive Decorrelation," in *Proc. 23rd IEEE Convention of Electrical and Electronics Engineers in Israel*, Sept. 2004, pp. 388–391.
- [3] J. Besag, "On the Statistical Analysis of Dirty Pictures," *Journal Royal Statistical Society (B)*, vol. 48, no. 3, pp. 259–302, 1986.
- [4] L. Rudin, S. Osher, and E. Fatemi, "Nonlinear Total Variation Based Noise Removal Algorithms," *Physica D*, vol. 60, pp. 259–268, 1992.
- [5] D.M. Strong, P. Blomgren, and T.F. Chan, "Spatially Adaptive Local Feature-Driven Total Variation Minimizing Image Restoration," in *Proceedings of SPIE., Statistical and Stochastic Methods in Image Processing II*, Oct. 1997, vol. 3167, pp. 222–233.
- [6] A. Tonazzini, L. Bedini, E.E. Kuruoglu, and E. Salerno, "Blind Separation of Auto-Correlated Images from Noisy Mixtures Using MRF Models," in *ICA 2003*, Apr. 2003, pp. 675–680.